Soluble n-type pentacene derivatives as novel acceptors for organic solar cells†

Yee-Fun Lim,‡[a] Ying Shu,‡[b] Sean R. Parkin,[b] John E. Anthony*[b] and George G. Malliaras*[a]

Received 22nd October 2008, Accepted 3rd February 2009
First published as an Advance Article on the web 17th March 2009
DOI: 10.1039/b818693f

6,13-Bis(triisopropylsilylethynyl) (TIPS)-pentacene has proven to be a promising soluble p-type material for organic thin film transistors as well as for photovoltaics. In this work, we show that adding electron-withdrawing nitrile functional groups to TIPS-pentacene turns it into an n-type material, which can be used as an acceptor for organic solar cells. Several new cyanopentacenes with different trialkylsilyl functional groups have been synthesized. The HOMO–LUMO energy levels can be tuned by varying the number of nitrile groups, while the trialkylsilyl groups control crystal packing and film morphology. Solar cells were fabricated from a blend of poly(3-hexylthiophene) (P3HT) as the donor and the cyanopentacenes as acceptors, and we found that the acceptors that stack in a 1D "sandwich-herringbone" exhibited the best performance of derivatives in this study. A solar cell fabricated from a blend of P3HT and 2,3-dicyano-6,13-bis-(tricyclopentylsilylethynyl) pentacene (2,3-CN2-TCPS-Pn) exhibited a power conversion efficiency of 0.43% under 100 mW cm^{-2} AM 1.5 illumination.

1. Introduction

Organic solar cells (OSCs) promise energy production at reduced cost, since they can be fabricated by low-cost methods such as roll-to-roll processes.[1] Blends of poly(3-hexylthiophene) (P3HT) and [6,6]-phenyl-C_{61} butyric acid methyl ester (PCBM) represent one of the most efficient OSC material sets, yielding efficiencies of 5%.[2] The success of PCBM as a champion acceptor for OSCs is due to its ability to accept electrons from semiconducting polymers at ultrafast ($\sim 10^{-12}$ s) time scales,[3] and the nano-scale interpenetrating network that it forms with these polymers.[4] However, PCBM suffers from disadvantages including high energy costs for material production and poor absorption in the visible spectrum.[5] Excited fullerene states are also known to produce highly reactive singlet oxygen,[5] which can lead to device degradation in air.

Besides PCBM and other fullerene derivatives, efficient OSCs have been fabricated predominantly from polymer acceptors, with best reported efficiencies around 1.8%.[6] Polymer acceptors have the advantages of good absorption in the visible region and a higher LUMO energy level than PCBM, giving rise to a higher open-circuit voltage (V_{OC}).[6] The polydispersity of polymers, however, increases fabrication complexity since performance has been shown to be correlated to molecular weight.[7] Electron transport in some polymer acceptors is trap-limited,[8] which reduces fill factor and lowers efficiency. It is therefore desirable to search for alternative n-type small molecule acceptors. Recently, it has been reported that solar cells with Vinazene derivatives as small molecule acceptors achieved efficiencies as high as 0.75%.[9]

6,13-Bis(triisopropylsilylethynyl) (TIPS)-pentacene is a promising p-type organic semiconductor for use in organic thin film transistors (OTFTs)[10] and OSCs.[11] TIPS-pentacene is soluble in common organic solvents, exhibits excellent 2D π-stacking,[12] high hole mobility (>1 $cm^2 V^{-1} s^{-1}$),[10] and good absorption in the visible region.[11] When combined with the acceptor C_{60} in a bilayer configuration, a solar cell efficiency of 0.52% was achieved.[11] It has been reported that the addition of nitrile functional groups to this molecule reduces its HOMO–LUMO energy levels,[13] which raises the intriguing possibility of it being used as an n-type acceptor in OSCs. The cyanation of acenes has also been theorized to promote π-stacking and decrease internal reorganization energy.[14]

In this work, we report on the synthesis of various cyanopentacenes, and their solar cell performance when blended with P3HT as a donor. Crystal packing and film morphology are changed by modifying the trialkylsilyl group, while varying the number of nitrile groups alters the HOMO–LUMO energy levels. This tunability is highly desirable since a recent study shows that OSC efficiency is strongly dependent on the relative HOMO–LUMO energy levels between donor and acceptor.[15] Our results show that cyanopentacenes can be employed as OSC acceptors, with efficiencies up to 0.43%.

[a]*Department of Materials Science and Engineering, Cornell University, Ithaca, NY, 14850, USA. E-mail: ggm1@cornell.edu; Fax: +1 607 255 2365; Tel: +1 607 255 1956*
[b]*Department of Chemistry, University of Kentucky, Lexington, KY, 40506, USA. E-mail: anthony@uky.edu; Fax: +1 859 323 1069; Tel: +1 859 257 8844*

† CCDC reference numbers 722603–722606. For crystallographic data in CIF or other electronic format see DOI: 10.1039/b818693f

‡ These authors contributed equally to this work.

2. Experimental

2.1 Synthetic details

General. Bulk solvents (hexanes, dichloromethane, and acetone) were purchased from Pharmco-Aaper. Dry THF was purchased from Aldrich. Commercial acetylene (TIPS) was purchased from GFS Chemicals. Silica gel 230–400 mesh was bought from Sorbent Technologies. NMR spectra were measured on a Varian (Gemini 200 MHz) spectrometer, chemical shifts were reported in ppm relative to $CDCl_3$ as an internal standard. Mass spectroscopy was performed by laser-desorption ionization (LDI) on a JEOL (JMS-700 T) Mass Spectrometer. Differential scanning calorimetry (DSC) was performed using an N_2-purged Mettler DSC 822_e with a scan rate of 10 °C min^{-1}.

General procedure for the preparation of cyanopentacenes. The synthesis of trialkylsilylethynyl-substituted cyanopentacenes (Fig. 1) began by the condensation of 4,5-diiodobenzene-1,2-dicarbaldehyde[16] with either 1,4-cyclohexanedione or 1,4-dihydroxyanthracene to yield tetraiodo or diiodo pentacenequinone. Ethynyllithium solutions were prepared by treatment of the alkyne with nBuLi in THF for 1 h, followed by addition of the diiodo or tetraiodo pentacenequinone. After the quinone was fully dissolved, the reaction was quenched with saturated ammonium chloride solution, the crude diol was isolated *via* silica chromatography (hexanes–dichloromethane 4 : 1 v/v). Deoxygenation of the diol proceeded *via* the Miao–Bunz deoxygenation method,[17] and the resulting trialkylsilylethynyl iodopentacenes were recrystallized from hexanes. The trialkylsilylethynyl iodopentacenes were then treated with potassium cyanide in the presence of a palladium(0) catalyst and CuI in THF at 80 °C for 16 h to yield the desired cyanopentacenes. The reaction products were purified first by chromatography (hexanes–dichloromethane 1 : 1 v/v). Compounds **1a–1d** were then recrystallized from acetone, **2a** was recrystallized from dichloromethane, and **3c** was recrystallized from hexanes. Monocyano TCPS pentacene (**3c**) was obtained as a reaction byproduct from the cyanation of diiodo TCPS pentacene. For clarity, the molecular structures of the cyanopentacenes are shown in Fig. 2.

*2,3-Dicyano-6,13-bis-(triisopropylsilylethynyl)pentacene (2,3-CN2-TIPS-Pn) (**1a**).* ^{1}H NMR (200 MHz, $CDCl_3$): δ 9.38 (2H, s), 9.33 (2H, s), 8.43 (2H, s), 7.99 (2H, dd, J = 3.0, 6.2 Hz), 7.48 (2H, dd, J = 3.0, 6.6 Hz), 1.36 (42H, s). ^{13}C NMR (50 MHz, $CDCl_3$): δ 138.8, 133.2, 131.5, 131.3, 129.7, 128.9, 128.7, 127.1, 126.8, 120.1, 116.2, 109.7, 108.1, 103.4, 19.0, 11.6. MS (LDI) *m/z* 688 (100%, M^+). Decomposition temperature: 350 °C.

*2,3-Dicyano-6,13-bis-(triisobutylsilylethynyl)pentacene (2,3-CN2-TIBS-Pn) (**1b**).* ^{1}H NMR (200 MHz, $CDCl_3$): δ 9.34 (2H, s), 9.29 (2H, s), 8.42 (2H, s), 7.92 (2H, dd, J = 3.2, 6.6 Hz), 7.39 (2H, dd, J = 3.4, 6.8 Hz), 2.16 (6H, sept, J = 7.4 Hz), 1.16

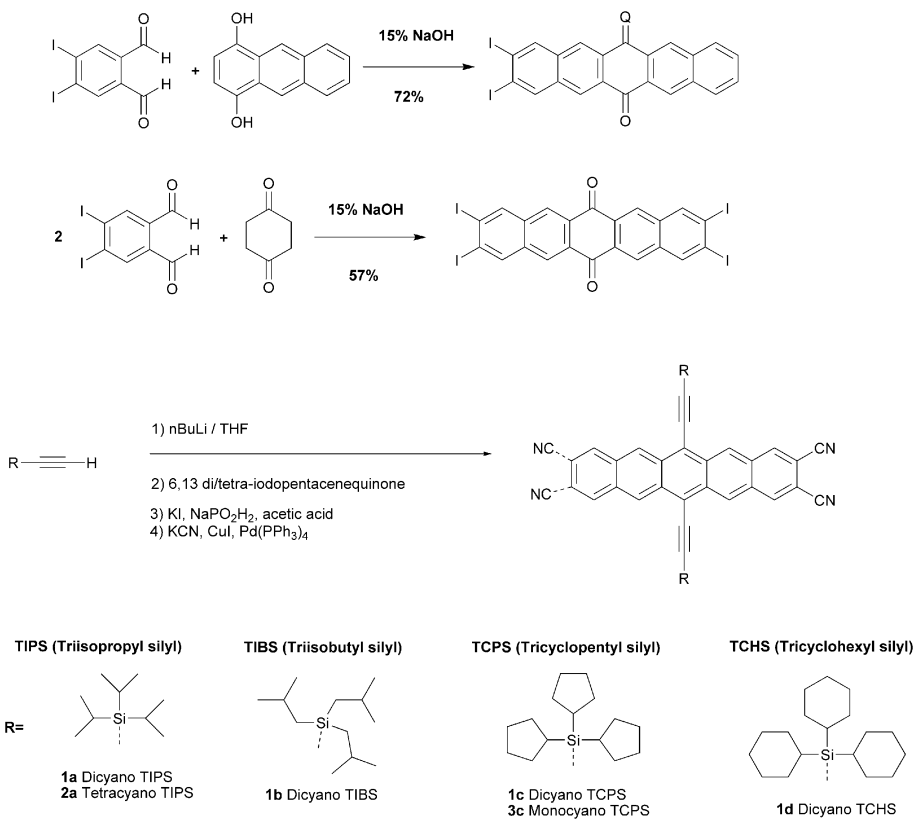

Fig. 1 The synthesis of functionalized cyanopentacenes.

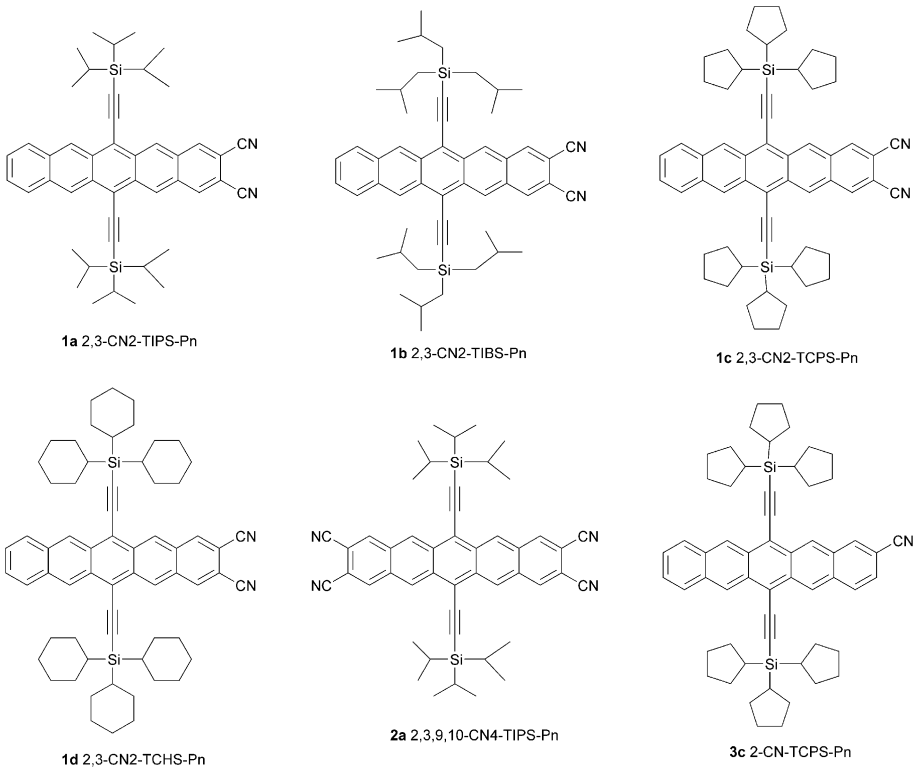

Fig. 2 Molecular structures of the cyanopentacenes.

(21H, d, $J = 6.6$ Hz), 0.98 (12H, d, $J = 7.0$ Hz). ^{13}C NMR (50 MHz, $CDCl_3$): δ 138.8, 133.5, 131.8, 131.6, 129.8, 129.2, 128.8, 127.4, 127.0, 120.3, 116.4, 112.6, 108.5, 103.7, 26.7, 25.6, 25.5. MS (LDI) *m/z* 772 (100%, M^+). Decomposition temperature: 245 °C.

*2,3-Dicyano-6,13-bis-(tricyclopentylsilylethynyl)pentacene (2,3-CN2-TCPS-Pn) (**1c**).* ^{1}H NMR (200 MHz, $CDCl_3$): δ 9.34 (2H, s), 9.29 (2H, s), 8.42 (2H, s), 7.98 (2H, dd, $J = 3.4$, 6.6 Hz), 7.50 (2H, dd, $J = 3.4$, 6.6 Hz), 2.05 (12H, m), 1.72 (36H, m), 1.36 (6H, m). ^{13}C NMR (50 MHz, $CDCl_3$): δ 139.0, 133.5, 131.8, 131.6, 130.0, 129.2, 128.9, 127.4, 120.4, 116.4, 110.6, 108.5, 102.8, 29.6, 27.3, 24.0. MS (LDI) *m/z* 844 (100%, M^+). Decomposition temperature: 265 °C.

*2,3-Dicyano-6,13-bis-(tricyclohexylsilylethynyl)pentacene (2,3-CN2-TCHS-Pn) (**1d**).* ^{1}H NMR (200 MHz, $CDCl_3$): δ 9.37 (2H, s), 9.33 (2H, s), 8.41 (2H, s), 7.99 (2H, dd, $J = 3.6$, 6.6 Hz), 7.48 (2H, dd, $J = 3.6$, 6.8 Hz), 2.03 (12H, m), 1.83 (18H, m), 1.56 (9H, m), 1.26 (27H, m). ^{13}C NMR (50 MHz, $CDCl_3$): δ 139.0, 133.5, 131.9, 131.7, 130.1, 129.2, 128.9, 127.4, 127.2, 120.4, 116.4, 110.6, 108.5, 104.0, 29.2, 28.6, 27.2, 23.7. MS (LDI) *m/z* 929 (100%, M^+). Melting point: 265 °C.

*2,3,9,10-Tetracyano-6,13-bis-(triisopropylsilylethynyl)pentacene (2,3,9,10-CN4-TIPS-Pn) (**2a**).* ^{1}H NMR (200 MHz, $CDCl_3$): δ 9.43 (4H, s), 8.48 (4H, s), 1.54 (6H, s), 1.36 (36H, s). ^{13}C NMR (50 MHz, $CDCl_3$): δ 138.6, 132.9, 130.1, 129.9, 121.6, 115.8, 112.49, 109.4, 102.4, 19.1, 11.6. MS (LDI) *m/z* 738 (100%, M^+). Decomposition temperature: 260 °C.

*2-Cyano-6,13-bis-(tricyclopentylsilylethynyl)pentacene (2-CN-TCPS-Pn) (**3c**).* ^{1}H NMR (200 MHz, $CDCl_3$): δ 9.32 (4H, m), 8.36 (1H, s), 8.01 (3H, m), 7.47 (3H, m), 2.07 (12H, m), 1.81 (36H, m), 1.42 (6H, m). ^{13}C NMR (50 MHz, $CDCl_3$): δ 137.0, 133.1, 133.0, 131.6, 130.6, 130.4, 128.9, 127.5, 126.9, 126.8, 124.7, 119.8, 119.6, 119.2, 109.7, 109.6, 109.1, 103.5, 103.4, 29.6, 27.3, 24.1. MS (LDI) *m/z* 844 (100%, M^+). Decomposition temperature: 275 °C.

*Crystal data for compound **1d**.* $C_{64}H_{74}N_2Si_2$, $M = 927.43$, orthorhombic, $a = 16.6409(6)$, $b = 17.5827(7)$, $c = 18.8903(8)$ Å, $\alpha = 90.00°$, $\beta = 90.00°$, $\gamma = 90.00°$, $V = 5527.1$ Å^3, $T = 90.0(2)$ K, space group *Pnma*, $Z = 4$, 6945 reflections measured, 3748 unique ($R_{int} = 0.0763$), $R1[I > 2\sigma(I)] = 0.0881$.

*Crystal data for compound **3c**.* $C_{55}H_{64}NSi_2$, $M = 795.25$, orthorhombic, $a = 16.8241(6)$, $b = 17.0411(9)$, $c = 16.1283(7)$, $\alpha = 90.00°$, $\beta = 90.00°$, $\gamma = 90.00°$, $V = 4624.0(4)$ Å^3, $T = 90.0(2)$ K, space group *Pnma*, $Z = 4$, 65241 reflections measured, 4431 unique ($R_{int} = 0.0796$), $R1[I > 2\sigma(I)] = 0.1142$.

*Crystal data for compounds **1a** and **2a**.* Taken from ref. 13, are available from the Cambridge Structural Database, RefCodes TATLEG and TATLIK, respectively.

2.2 Device fabrication

Solar cells were fabricated on pre-patterned indium tin oxide (ITO) coated glass substrates (Kintec, Hong Kong), which were cleaned by sonication in a mild detergent, rinsed in de-ionized

water, dried in a nitrogen stream, and treated with a 10 min UV–ozone exposure. PEDOT:PSS (Baytron P from H. C. Starck) was filtered through a 0.45 μm PVDF syringe filter, and then deposited by spin-coating at 6000 rpm for 60 s. The PEDOT:PSS layer was baked on a hotplate at 170 °C for 4 min to remove residual solvent. The samples were then transferred into a nitrogen-filled glovebox, in which all subsequent processing steps were carried out.

P3HT (American Dye Source) and the cyanopentacenes were dissolved in toluene at a ratio of 1 : 1 by weight to give a total concentration of 20 mg ml^{-1}. This ratio was initially kept constant for all derivatives to allow for easy comparison, but was later optimized for the best performing derivatives. The solutions were allowed to stir in the glovebox overnight, before they were spin-coated on top of the PEDOT:PSS layer at 1000 rpm for 60 s. All films were then annealed on a hotplate at 160 °C for 8 min, except for 2-CN-TCPS-Pn (**3c**) since solar cells made from this material were found to degrade under thermal treatment. Finally, 4 Å of CsF and 400 Å of Al were thermally evaporated under high vacuum ($\sim 10^{-6}$ Torr) to form the cathode for the devices. A shadow mask was used in the evaporation to define a device active area of 3 mm^2. Control P3HT:PCBM solar cells were also fabricated according to a previously published recipe.[18]

3. Results and discussion

3.1 Crystallography

Two of the most common crystal packing motifs for acenes used as organic semiconductors are the edge-to-face "herringbone" arrangement and the face-to-face π-stacking arrangement.[14] Trialkylsilylethynyl substitution on acenes generally yields 1D and 2D π-stacked arrays.[19] While we have found that 2D "brickwork" stacking motifs (such as that of 2,3-CN2-TIPS-Pn (**1a**)—Fig. 3, top left) yield the best transport in planar devices such as transistors,[12] molecules with these packing arrangements perform poorly in OSC device studies (see Section 3.3 and Table 2). Crystallographic studies of pentacene derivatives with larger trialkylsilyl substituents are complicated by the tendency for disorder in these groups. A poorly refined structure for 2,3-CN2-TIBS-Pn (**1b**) suggests packing similar to the TIPS derivative (**1a**), and the poor performance of this material in OSC devices lends support to this assignment. Similar poor performance was also observed in 2,3,9,10-CN4-TIPS-Pn (**2a**) which adopts a 1D "slipped-stack" motif. Cyanopentacenes **1d** and **3c** both adopt a "sandwich-herringbone" motif (Fig. 3, right), and are among the best-performing materials in our studies. While the crystal structure of the TCPS derivative **1c** could not be fully resolved, again due to extensive disorder, the collected data do support a gross packing similar to **1d** and **3c**, and the film morphology and device performance (see Section 3.3) of this compound are closely related.

3.2 Electrochemistry

Differential pulse voltammetry was performed with a BAS CV-50 W voltammetric analyzer at room temperature with a platinum button working electrode, a platinum wire counter electrode and a silver wire pseudo-reference electrode, in a nitrogen-purged 0.1 M Bu_4NPF_6 solution in dichloromethane, using ferrocene/ferrocenium as an internal standard at a scan rate of 20 mV s^{-1}. All values quoted are relative to Fc/Fc^+ (Table 1).

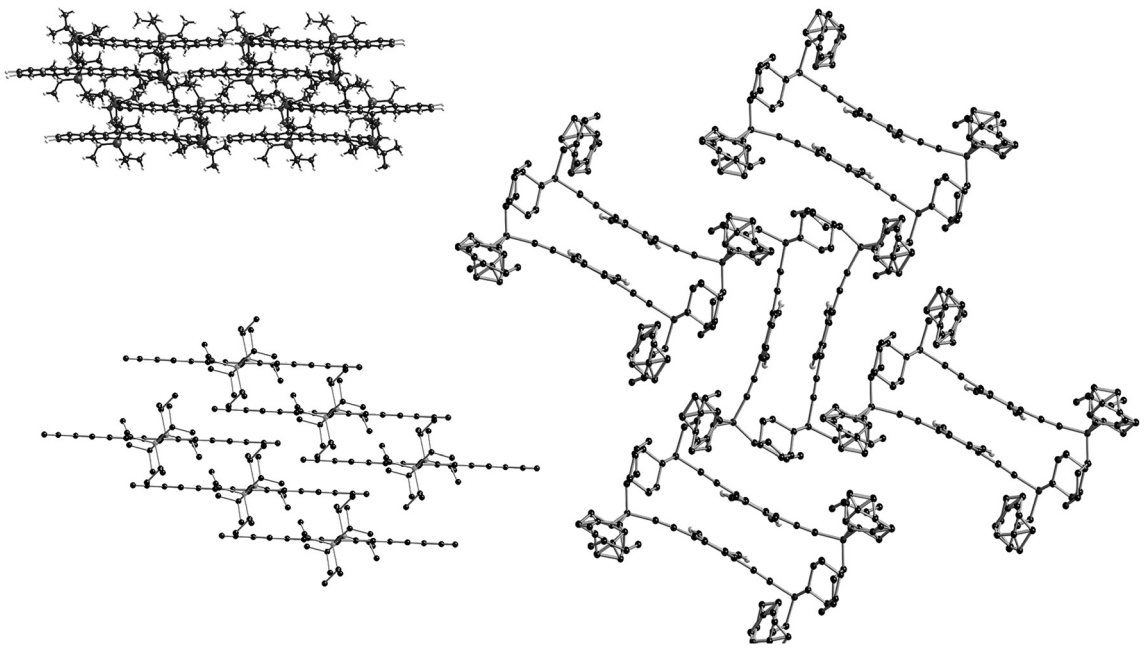

Fig. 3 Representative crystal packings of the cyanopentacenes. Top left: 2,3-CN2-TIPS-Pn (**1a**), showing a strong 2D "brickwork" packing. Bottom left: 2,3,9,10-CN4-TIPS-Pn (**2a**). Right: 2,3-CN2-TCHS-Pn (**1d**). In contrast to the 2D π stacks of 2,3-CN2-TIPS-Pn (**1a**), the acene faces of 2,3,9,10-CN4-TIPS-Pn (**2a**) adopt a 1D π stack arrangement. Cyanopentacenes with larger trialkylsilyl groups, such as 2,3-CN2-TCHS-Pn (**1d**) and 2-CN-TCPS-Pn (**3c**), arrange themselves in a "sandwich-herringbone" motif (right).

Table 1 Electrochemical data[a]

Material	E_{ox}/mV	E_{red1}/mV	E_{red2}/mV	E_{gap}/mV
2,3-CN2-TIPS-Pn (**1a**)	644	−1174	−1593	1818
2,3-CN2-TIBS-Pn (**1b**)	636	−1164	−1623	1800
2,3-CN2-TCPS-Pn (**1c**)	666	−1156	−1565	1820
2,3-CN2-TCHS-Pn (**1d**)	649	−1170	−1612	1819
2,3,9,10-CN4-TIPS-Pn (**2a**)	954	−895	−1429	1849
2-CN-TCPS-Pn (**3c**)	509	−1300	N/A	1809
TIPS-pentacene	363	−1451	N/A	1814
P3HT	363	N/A	N/A	N/A

[a] Differential pulse voltammetry was performed in a 0.1 M solution of Bu_4NPF_6 in dichloromethane, with a Pt working electrode, a scan rate of 20 mV s^{-1}, and ferrocene as an internal standard.

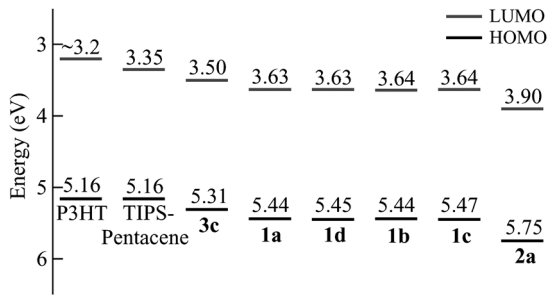

Fig. 4 HOMO–LUMO energy levels calculated from electrochemical data.

HOMO–LUMO energy levels are calculated from the electrochemical data and plotted in Fig. 4.

The sequential addition of nitrile groups to the pentacene core raises both the oxidation and reduction potentials of the material. However, neither the number of nitrile groups on the acene core nor changes in the configuration of the trialkylsilyl group yield significant changes in the HOMO–LUMO gap of the pentacene. A reversible oxidation and two reversible reductions were seen for all cyanopentacenes except for 2-CN-TCPS-Pn (**3c**), which exhibited only one reversible reduction in the window scanned (±1.8 V). No significant differences in redox potentials were observed between any of the dicyano pentacenes, indicating that energy levels are not altered by the various trialkylsilylethynyl substitutions, and only by electron-withdrawing nitrile groups on the pentacene core. No reduction potentials were seen for P3HT, and the LUMO is estimated from the optical band gap.

3.3 Solar cell *I–V* characterization

Current–voltage (*I–V*) curves were obtained with a Keithley 236 source-measurement-unit (SMU) under AM 1.5 100 mW cm^{-2} illumination from a Solar Light 16S-002 solar simulator. Light output power was calibrated using a Newport 818P-010-12 thermopile high power detector, which has a flat response over a broad spectral range. Spectral mismatch was not taken into account in these measurements.

The solar cell performance of the various cyanopentacene derivatives is shown in Table 2. The open-circuit voltage (V_{OC}), short circuit current (J_{SC}), fill factor (FF) and power conversion efficiency (PCE) are reported, together with the crystal stacking. As mentioned above, all cells reported here have 1 : 1 donor–acceptor ratios by weight. V_{OC} values were quite satisfactory, and a V_{OC} as high as 0.82 V was achieved for 2-CN-TCPS-Pn (**3c**). This is higher than the V_{OC} of P3HT:PCBM cells, for instance, which is reported to be around 0.6 V.[2] However, J_{SC} and PCE values were not as impressive, and the best performing acceptor is 2,3-CN2-TCPS-Pn (**1c**) with a modest PCE of 0.43%.

Optical microscopy was used to probe film morphology of these pentacene derivatives. Fig. 5(a) shows a film spin-cast from a 1 : 1 blend of P3HT and 2,3-CN2-TIPS-Pn (**1a**), showing the formation of large (~10–20 μm) crystals. In fact, we observed that the films appeared cloudy after spin-coating, due to light scattering from these crystals. Since it is desirable to have donor–acceptor domains of ~10 nm in size for efficient exciton dissociation to occur,[4] the large scale phase separation observed here is the likely cause of the low J_{SC} and PCE of these cells. Strong inter-molecular interactions due to 2D π-stacking may be the reason for the formation of such large crystals. In contrast, a film spin-coated from a P3HT:2,3-CN2-TCPS-Pn solution does not exhibit large crystal formation (Fig. 5(b)), probably due to weaker π-stacking interactions in the solid state. Therefore, such materials may produce a better film morphology for exciton dissociation. This general observation was noted over all of the 1D and 2D π-stacking materials examined in this study. Hence, similar to our observation with anthradithiophene-based donors,[20] OSCs show the opposite trend as compared to OTFTs, for which 2D π-stacking materials were found to give the highest transistor mobilities.[12]

The HOMO–LUMO energy levels of the cyanopentacenes can explain the differences in the V_{OC}. It has been reported that the V_{OC} is approximately related to the energy levels by the following relationship:

$$V_{OC} = (1/e)\left(\left|E^{\text{donor}}\text{HOMO}\right| - \left|E^{\text{acceptor}}\text{LUMO}\right|\right) - 0.3\ \text{V}$$

Table 2 Solar cell performance from a 1 : 1 donor–acceptor blend

Acceptor	Stacking	V_{OC}/V	J_{SC}/mA cm^{-2}	FF	PCE (%)
2,3-CN2-TIPS-Pn (**1a**)	2D "brickwork"	0.58	0.44	0.38	0.10
2,3-CN2-TIBS-Pn (**1b**)	2D "brickwork"	0.50	0.67	0.37	0.12
2,3-CN2-TCPS-Pn (**1c**)	1D "sandwich-herringbone"	0.54	1.93	0.41	0.43
2,3-CN2-TCHS-Pn (**1d**)	1D "sandwich-herringbone"	0.60	1.16	0.38	0.26
2,3,9,10-CN4-TIPS-Pn (**2a**)	1D "slipped-stack"	0.44	0.36	0.40	0.06
2-CN-TCPS-Pn (**3c**)	1D "sandwich-herringbone"	0.82	1.11	0.34	0.31

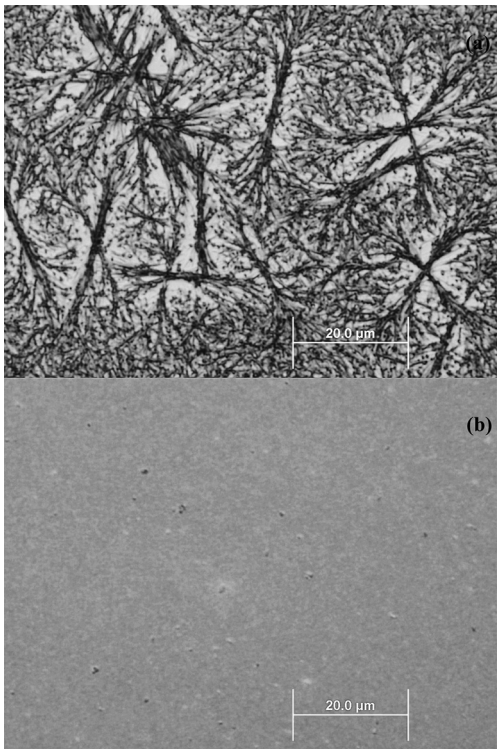

Fig. 5 Optical microscope images of (a) a P3HT:2,3-CN2-TIPS-Pn film and (b) a P3HT:2,3-CN2-TCPS-Pn film. Scale bars indicate 20 μm.

where e is the electron charge and the 0.3 V voltage "loss" is an empirical value.[15] Hence, a larger difference between the donor HOMO and the acceptor LUMO energy levels will lead to higher V_{OC}. By comparing the energy levels in Fig. 4 and the V_{OC} values in Table 2, it is clear that this trend is observed, and it is not surprising that the highest V_{OC} was obtained with 2-CN-TCPS-Pn (**3c**) which has the lowest absolute LUMO value of 3.50 eV. The ability to tune HOMO–LUMO energy levels of the cyanopentacenes is thus a great advantage of this family of acceptors, since it allows control of the V_{OC}.

Some optimization was carried out on 2-CN-TCPS-Pn (**3c**) and 2,3-CN2-TCPS-Pn (**1c**), which are the two best performing

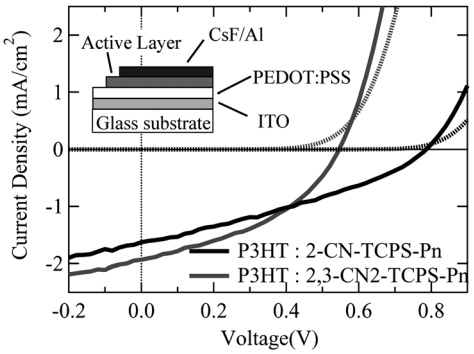

Fig. 6 I–V curves of the optimized devices in the dark (dashed curves) and under AM 1.5 100 mW cm^{-2} illumination (solid curves). The device structure is shown in the inset.

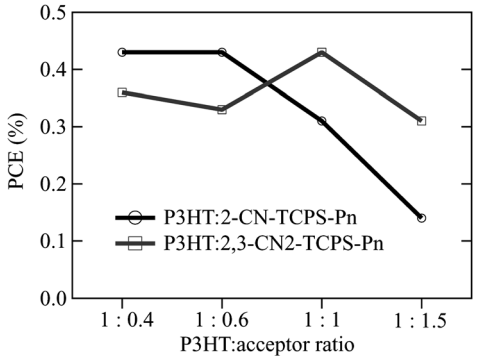

Fig. 7 Effect of donor–acceptor ratio on PCE.

acceptors in this study. The original 1 : 1 blend ratio was found to be the best for the P3HT:2,3-CN2-TCPS-Pn system, and the optimized cell achieved a 0.54 V V_{OC}, 1.93 mA cm^{-2} J_{SC}, 0.41 FF and 0.43% PCE. With regards to the P3HT:2-CN-TCPS-Pn system, a 1 : 0.4 donor–acceptor blend gave the best performance with a 0.78 V V_{OC}, 1.63 mA cm^{-2} J_{SC}, 0.34 FF and 0.43% PCE. The optimized I–V curves are plotted in Fig. 6. The efficiencies of cells as a function of donor–acceptor blend ratios are plotted in Fig. 7. In comparison, the control P3HT:PCBM cell achieved a 0.64 V V_{OC}, 10.31 mA cm^{-2} J_{SC}, 0.61 FF and 4.05% PCE, which is significantly better than the best cyanopentacene cells. Work is in progress to further improve the performance of the cyanopentacenes.

3.4 UV-Vis absorption and external quantum efficiency

UV-Vis absorption spectra were obtained using a Shimadzu UV-3101PC UV/Vis/Near-IR Spectrophotometer. The absorption spectra of P3HT, PCBM, and the two best performing acceptors are shown in Fig. 8. PCBM does not absorb significantly in the visible, while P3HT has good absorption up to about 650 nm. The cyanopentacene acceptors absorb further into the red, with 2,3-CN2-TCPS-Pn (**1c**) exhibiting an absorption peak at 700 nm. The cyanopentacenes thus have the potential to extend the spectral response of P3HT-based solar cells. To verify this claim, external quantum efficiency (EQE)

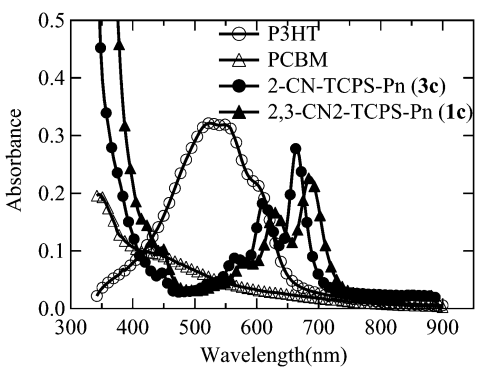

Fig. 8 UV-Vis absorption spectra comparison between P3HT, PCBM, and the best performing cyanopentacene derivatives.

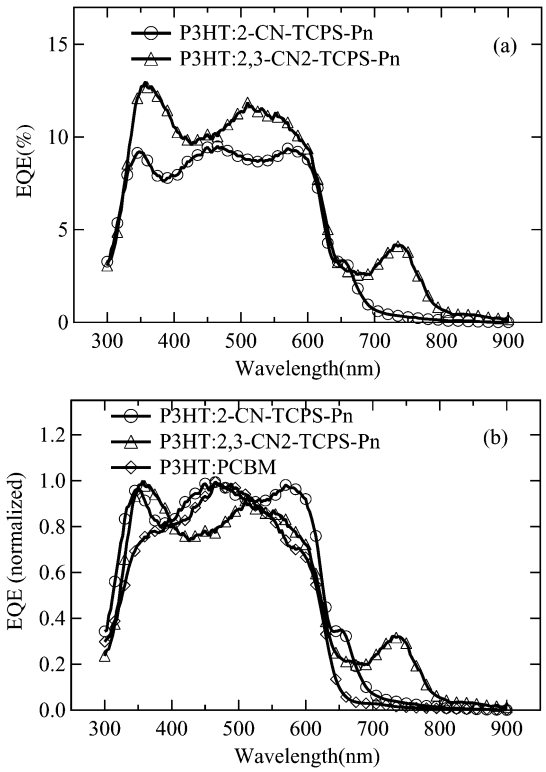

Fig. 9 External quantum efficiency (EQE) measurements. (a) Absolute EQE values for the best performing cells. (b) Normalized EQE curves for comparison with P3HT:PCBM.

spectra were obtained for the best performing cells. The EQE measurements were performed using a Newport 1000 W xenon lamp coupled to an Oriel Cornerstone 260 ¼ m monochromator as the light source, a Keithley 236 SMU to measure short circuit current, and a Newport 918D-UV3-OD3 low power detector to monitor the light intensity. Fig 9(a) shows the absolute EQE values, and the P3HT:2,3-CN2-TCPS-Pn cell achieved an EQE of 3–4% in the 700–750 nm spectral region. The EQE spectrum is red-shifted with respect to the absorption spectrum, which is likely due to further crystallization upon thermal annealing. Since P3HT does not absorb beyond 650 nm, this contribution to the photocurrent must be attributed to the acceptor. The EQE values were normalized and plotted in Fig. 9(b), in order to provide a comparison with the P3HT:PCBM system (which has a peak EQE of about 75% at 500 nm). The normalized EQE spectra clearly demonstrate that the cyanopentacene cells have a photovoltaic response extending further into the red, hence capturing a larger fraction of the solar spectrum.

4. Conclusions

Cyanopentacenes have demonstrated potential as a new class of acceptors for OSCs, with PCE up to 0.43% and absorption λ_{max} beyond 700 nm. While the efficiencies are still low when compared to a champion system such as P3HT:PCBM, it is possible to independently tune both the HOMO–LUMO energy levels (cyano substitution) and film morphology (trialkylsilyl substitution) of the cyanopentacenes. Hence there is significant substitution space available to optimize the material. Guiding this search will be the finding that molecules with a "sandwich-herringbone" 1D π-stacking arrangement (*e.g.* **1d**, **3c**) can yield devices with better performance than those exhibiting a 2D arrangement (**1a**). We are optimistic that this class of materials can eventually perform much better than the best efficiencies reported here.

Acknowledgements

This work was supported by a grant from the Office of Naval Research (ONR). Yee-Fun Lim acknowledges a fellowship from the Agency of Science, Technology and Research (A*STAR), Singapore. Ying Shu would like to thank her co-worker Mr Balaji Purushothaman for his generosity in providing TCPS and TCHS alkynes.

References

1 G. Dennler and N. S. Sariciftci, *Proc. IEEE*, 2005, **93**, 1429–1439; C. J. Brabec and J. R. Durrant, *MRS Bull.*, 2008, **33**, 670–675.
2 G. Li, V. Shrotriya, J. Huang, Y. Yao, T. Moriarty, K. Emery and Y. Yang, *Nat. Mater.*, 2005, **4**, 864–868; M. Reyes-Reyes, K. Kim, J. Dewald, R. Lopez-Sandoval, A. Avadhanula, S. Curran and D. L. Carroll, *Org. Lett.*, 2005, **7**, 5749–5752; W. Ma, C. Yang, X. Gong, K. Lee and A. J. Heeger, *Adv. Funct. Mater.*, 2005, **15**, 1617–1622.
3 N. S. Sariciftci, L. Smilowitz, A. J. Heeger and F. Wudl, *Science*, 1992, **258**, 1474–1476; G. Yu, J. Gao, J. C. Hummelen, F. Wudl and A. J. Heeger, *Science*, 1995, **270**, 1789–1791.
4 X. Yang, J. Loos, S. C. Veenstra, W. J. H. Verhees, M. M. Wienk, J. M. Kroon, M. A. J. Michels and R. A. J. Janssen, *Nano Lett.*, 2005, **5**, 579–583.
5 R. Koeppe and N. S. Sariciftci, *Photochem. Photobiol. Sci.*, 2006, **5**, 1122–1131.
6 S. C. Veenstra, J. Loos and J. M. Kroon, *Prog. Photovoltaics*, 2007, **15**, 727–740; T. Kietzke, H.-H. Horhold and D. Neher, *Chem. Mater.*, 2005, **17**, 6532–6537; C. R. McNeill, A. Abrusci, J. Zaumseil, R. Wilson, M. J. McKiernan, J. H. Burroughes, J. J. M. Halls, N. C. Greenham and R. H. Friend, *Appl. Phys. Lett.*, 2007, **90**, 193506.
7 A. M. Ballantyne, L. Chen, J. Dane, T. Hammant, F. M. Braun, M. Heeney, W. Duffy, I. McCulloch, D. D. C. Bradley and J. Nelson, *Adv. Funct. Mater.*, 2008, **18**, 2373–2380.
8 M. M. Mandoc, B. de Boer and P. W. M. Blom, *Phys. Rev. B*, 2006, **73**, 155205; M. M. Mandoc, F. B. Kooistra, J. C. Hummelen, B. de Boer and P. W. M. Blom, *Appl. Phys. Lett.*, 2007, **91**, 263505.
9 R. Y. C. Shin, T. Kietzke, S. Sudhakar, A. Dodabalapur, Z.-K. Chen and A. Sellinger, *Chem. Mater.*, 2007, **19**, 1892–1894; Z. E. Ooi, T. L. Tam, R. Y. C. Shin, Z. K. Chen, T. Kietzke, A. Sellinger, M. Baumgarten, K. Mullen and J. C. deMello, *J. Mater. Chem.*, 2008, **18**, 4619–4622.
10 S. K. Park, T. N. Jackson, J. E. Anthony and D. A. Mourey, *Appl. Phys. Lett.*, 2007, **91**, 063514.
11 M. T. Lloyd, A. C. Mayer, A. S. Tayi, A. M. Bowen, T. G. Kasen, D. J. Herman, D. A. Mourey, J. E. Anthony and G. G. Malliaras, *Org. Electron.*, 2006, **7**, 243–248.
12 J. E. Anthony, *Angew. Chem., Int. Ed.*, 2008, **47**, 452–483.
13 C. R. Swartz, S. R. Parkin, J. E. Bullock, J. E. Anthony, A. C. Mayer and G. G. Malliaras, *Org. Lett.*, 2005, **7**, 3163–3166.
14 M.-Y. Kuo, H.-Y. Chen and I. Chao, *Chem.–Eur. J.*, 2007, **13**, 4750–4758.
15 M. C. Scharber, D. Muhlbacher, M. Koppe, P. Denk, C. Waldauf, A. J. Heeger and C. J. Brabec, *Adv. Mater.*, 2006, **18**, 789–794.

16 J. Jiang, B. R. Kaafarani and D. C. Neckers, *J. Org. Chem.*, 2006, **71**, 2155–2158.
17 S. Miao, M. D. Smith and U. H. F. Bunz, *Org. Lett.*, 2006, **8**, 757–760.
18 K. Kim, J. Liu, M. A. G. Namboothiry and D. L. Carroll, *Appl. Phys. Lett.*, 2007, **90**, 163511.
19 J. Chen, S. Subramanian, S. R. Parkin, M. Siegler, K. Gallup, C. Haughn, D. C. Martin and J. E. Anthony, *J. Mater. Chem.*, 2008, **18**, 1961–1969.
20 M. T. Lloyd, A. C. Mayer, S. Subramanian, D. A. Mourey, D. J. Herman, A. V. Bapat, J. E. Anthony and G. G. Malliaras, *J. Am. Chem. Soc.*, 2007, **129**, 9144–9149.

